1966

The Modulated Absorption of Light in an Optical Pumping Experiment in 4He

Bruce Partridge
Haverford College, bpartrid@haverford.edu

G. W. Series

Follow this and additional works at: http://scholarship.haverford.edu/physics_facpubs

The modulated absorption of light in an optical pumping experiment on ^{4}He

The modulated absorption of light in an optical pumping experiment on 4He

R. B. PARTRIDGE† and G. W. SERIES

Clarendon Laboratory, Oxford

MS. received 1st March 1966

Abstract. Optical pumping experiments have been performed on helium 4 atoms in the metastable level $2\,^3S_1$ with the object of studying the modulation of light in absorption in the longitudinal and transverse beams. Magnetic resonance curves were obtained similar to those found in emission in double-resonance experiments. With a particular geometrical arrangement employing circular polarizers, the Bloch magnetic resonance curves were obtained.

Modulation at four times the applied frequency was obtained with a linear polarizer in the pumping beam. This modulation is ascribed to the circulation of coherence in the optical pumping cycle. From the behaviour of the resonance signals as a function of the frequency and amplitude of the stimulating field, it is inferred that a substantial part of the signal arises from coherence which has survived two complete cycles.

The observations are satisfactorily explained by the theory developed in the previous paper.

1. Introduction

Helium 4 provides a very convenient system for the study of the interactions between atoms and light. A mild discharge in the gas at a pressure of a few mmHg excites 10^{10}–10^{11} atoms/cm^3 to the metastable level $2\,^3S_1$. This serves as the ground level for optical pumping experiments. An aligned system may be obtained by illumination of the atoms with unpolarized or linearly polarized resonance radiation, 10 830 Å ($2\,^3S_1$–$2\,^3P_{0,1,2}$); circularly polarized radiation generates a partially polarized system.

The system was studied in detail by Colegrove and Franken (1960) and by Schearer (1961), with particular emphasis on the relaxation of the metastable atoms and on the possible applications to magnetometry. Its attractive feature as a system in which to study interaction processes is that it provides the counterpart in absorption to the much-studied mercury system, $6\,^1S_0$–$6\,^3P_1$, in emission (Brossel and Bitter 1952, Dodd, Series and Taylor 1963, Kibble and Series 1963, to be referred to respectively as DST and KS).

The similarities spring from the fact that both systems have the same angular momentum quantum number, namely 1, for the *initial* state of the optical transition. By magnetic resonance, the atoms can be prepared in superposition states of the Zeeman components $|m = 0, \pm 1\rangle$, and resonance phenomena studied in absorption or emission, as the case may be.

It is to be noticed that the light monitors magnetic resonance only if the resonance is taking place between the *initial* states of the optical transition. In the mercury system, for example, magnetic resonance in the excited states has a profound effect on the *emitted* light, but has no effect whatever on light *absorbed* by atoms in the same transition.

† Now at Palmer Physical Laboratory, Princeton University, Princeton, N.J., U.S.A.

To study effects in absorption similar to double resonance in emission, magnetic reson-ance must be stimulated in the lower states. This apparent lack of symmetry between the initial and final states in the optical transition will form the subject of a future communication.

Figure 1 shows the relevant transitions in helium and, for comparison, in mercury. The identity of the Zeeman structures of the initial states in the two systems leads to identity in the resonance phenomena as far as primary interactions are concerned, but the more complicated structure of the final states leads to a greater variety of phenomena in higher-order interactions in helium than is possible with mercury.
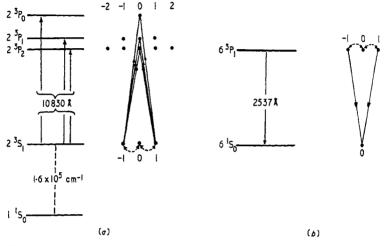

Figure 1. (a) Absorption of 10 830 Å in helium compared with (b) emission of 2537 Å in mercury. The structure of the initial level is the same in the two cases.

One further difference of experimental significance is that the initial state for helium is an S state, whereas for mercury it is a P state. The spherical symmetry of the S state implies that the directional properties of atoms in this state are determined entirely by the orientation of the spin. This is reflected in the intensity sum rules. The consequence is that the amount of light absorbed will be unaffected by magnetic resonance if the spectral density of the monitoring light is uniform over the spin multiplet. For this reason, the detection of magnetic resonance signals depends on inequalities of spectral density such as are normally found in helium lamps. The 10 830 Å radiation is usually emitted as a spectrally resolved doublet. The component ($^3S_1$–$^3P_0$) is resolved from, and weaker than, the blend ($^3S_1$–$^3P_1$, $^3P_2$). Colegrove and Franken (1960) and Schearer (1961) interpreted the vanishing of optical pumping signals under certain conditions as a consequence of the differential absorption of the components of the doublet.

Of the variety of effects studied with the helium system, we describe in this paper certain modulation phenomena, classified as α and β processes. These terms refer to the state of the system before the final interaction with the radio-frequency field. The atoms may have been left by previous cycles of optical pumping in eigenstates of the time-independent Hamiltonian, or in superposition states. The α processes are repre-sented by the further development of the eigenstates, and the β processes by the inter-ference terms which develop from the superposition states. In the language of density matrices, the α processes correspond to the development of the diagonal elements, and the β processes correspond to the development of the off-diagonal elements. This

classification represents a generalization of that used in DST and KS. α processes are the 'principal magnetic resonance phenomena', formerly described as case 1. Cases 2 and 3 were special cases of β processes.

The effects interpreted here as α processes include modulation effects at $2\omega_0$ in the pumping beam, and at ω_0 and $2\omega_0$ in a transverse beam ($\omega_0/2\pi$ is the applied radio frequency). In so far as similar effects were studied in the mercury system, the resonance curves found in helium were identical.

Modulation at frequencies higher than $2\omega_0$ cannot be due to α processes. In the present experiments, modulation at $4\omega_0$ was studied and ascribed to β processes. Such effects in optical pumping cycles are particularly interesting in that they prove that coherence between atomic eigenstates can survive the shock of optical excitation and the random isotropic perturbation which is responsible for spontaneous decay. That it can survive optical excitation has been shown by Skalinski and Rosinski (1964), who observed modulation at the ground-state resonance frequency in the fluorescent light from optically pumped sodium vapour. That coherence can be carried through a complete cycle of optical pumping was shown by Cohen-Tannoudji (1962) in studies of the transverse relaxation of mercury 199.

In the paper which follows (Partridge and Series 1966), it is shown that coherence between eigenstates can be transferred in collisions. The transfer of coherence in all these cases is governed by a condition of the type $\omega_f - \omega_i \gg \Gamma_f$, where ω_i and ω_f refer to the precessional frequencies of the initial and final states, and Γ_f is the damping constant of the final state. In physical terms, the requirement for the efficient transfer of coherence is that the precession of atoms in the initial and final states shall not develop a large phase difference within the mean lifetime of the final state.

The experimental results in this paper are compared with theoretical expressions derived in the preceding paper (Series 1966, to be referred to as I).

2. Experimental arrangements

The arrangements for securing optical pumping were similar to those described by Colegrove and Franken (1960). The disposition of apparatus is indicated in figure 1 of the following paper (Partridge and Series 1966).

The most favourable pressure of gas in the sample cells was $0 \cdot 1$–$0 \cdot 5$ mmHg. At pressures of this order there is very little relaxation by collision of atoms in the excited ^3P states. Barium getters were used in some of the cells.

The main magnetic field H was provided by Helmholtz coils of diameter $61 \cdot 5$ cm. Fields up to 1 G were used. Additional coils were used to provide low-frequency modulation and to compensate stray fields. Compensation was necessary to within 1 mG.

The frequency range in which the resonances were studied was limited by the response of the photodetector. For most experiments the frequency chosen ($\omega_0/2\pi$) was $0 \cdot 5$ or $1 \cdot 0$ kc/s. A rotating, rather than an oscillating, field was used, and was provided by two orthogonal pairs of Helmholtz coils of diameter 21 cm. Amplitudes H_1 up to 20 mG could be provided.

The system was monitored for modulation (a) in the pumping beam (z beam) with the use of linear or circular polarizers or analysers, and (b) transversely, (x beam) with an auxiliary lamp, using linear or circular polarizers.

The photoelectric detector was a semiconductor device (photo-duo-diode, Texas Instruments Ltd.); eight elements were used in parallel. These detectors can be used at frequencies up to 75 kc/s, but their response is independent of frequency only up to about 5 kc/s.

The photoelectric signals were taken through a tuned amplifier and displayed, either directly on an oscilloscope (using a time base synchronous with the low-frequency modulating field), or as the output of a phase-sensitive detector. In the latter case the reference signal was provided by the oscillator which generated H_1, with frequency multipliers for the harmonics. No additional low-frequency modulation was imposed. The output from the detector was taken to a pen recorder and plotted as a function of the field H. The experimental figures in this paper are plots of this sort. The field H was swept linearly through the resonances in times of the order of 100 sec. Integrating time constants up to 1 sec were employed.

Although the experiments were planned primarily for qualitative studies, some care was taken to ensure that the response of the recording system was linear to within a few per cent and the field sweep correspondingly uniform.

3. Experimental results

3.1. *General remarks*

3.1.1. *Use of polarizing filters.* Most of the results described below were obtained by using the pumping light to monitor the resonances (z-beam detection). It is to be realized that the use of polarizers in this case affects both the system studied and the monitoring beam. An analyser does not itself affect the system, but selects a component of the beam which has both pumped the sample and monitored it. In general, different results are obtained by placing a polarizing filter before or after the sample. This is not the case when the sample is monitored by an independent beam of light, provided that this is weak compared with the pumping beam. In such experiments it is immaterial on which side of the sample the filter is placed.

3.1.2. *Spurious signals.*

(i) *Elliptical radio-frequency field.* Many experiments were performed in which the frequency of resonance was less than the width of the resonance curves (15–30 kc/s). In such cases the counter-rotating component of an oscillating field cannot be ignored if comparisons are to be made with a simple theory of magnetic resonance such as is worked out in I. In the present experiments, certain spurious modulation effects were attributable to slight ellipticity in the rotating field.

(ii) *Elliptical polarizer.* Spurious modulation under other conditions was attributable to non-ideal circular polarizers. The proof of this was that the phase of the modulation changed systematically with the orientation of the polarizer.

(iii) *Off-axis light.* The use of light sources and detectors of finite size inevitably introduces departures from the ideal geometrical conditions. These were suspected of introducing spurious signals and investigated by the use of stops. It was found that off-axis light was not an important source of spurious signals.

3.1.3. *Vanishing of signals.* Colegrove and Franken (1960) pointed out that the vanishing of optical pumping signals (the unmodulated component of the transmitted light) for certain densities of metastable atoms was attributable to differential absorption of the components of the monitoring light. In the present experiments, modulation phenomena vanished under the same conditions as the optical pumping signals.

3.1.4. *Relative intensity of signals.* Magnetic resonance signals were studied in the unmodulated component of the transmitted light and in the components modulated at $2\omega_0$ and $4\omega_0$.

The strength of the unmodulated component under optimum conditions was less than 1% of the total amount of transmitted light.

The amplitude of the modulation at $2\omega_0$ at the peak of the resonance was approximately equal to the strength of the unmodulated component. The amplitude of the cosine component of modulation at $4\omega_0$ (symmetrical signal) was, under favourable conditions, comparable with that at $2\omega_0$. The amplitude of the sine component at $4\omega_0$ (antisymmetrical signal) was, under favourable conditions, about 5% of that of the symmetrical signal.

3.2. *Resonance functions*

Of the observed resonance curves, some were obtained under conditions such that only α processes would be expected; namely, with a circular polarizer or no polarizer in the pumping beam. These curves were compared with the functions A, B, C, D, E and F familiar from the double-resonance experiments (DST, KS), and with the Bloch functions

$$\chi' = \frac{b\delta}{\delta^2 + b^2 + \Gamma^2}, \qquad \chi'' = \frac{b\Gamma}{\delta^2 + b^2 + \Gamma^2}. \tag{1}$$

These latter were not obtained in the mercury system, though there is no reason to believe that they could not have been found there had they been sought under the right conditions.

With a linear polarizer in the pumping beam both α and β processes are expected. The additional signals found under these conditions were compared with the function F, and with the more complicated functions described in section 4 of I. Details of the comparisons are given below.

3.3. *Observation of α processes*

3.3.1. *Monitoring in the z direction.* Resonances were found according to table 1. The conditions stated are typical, but do not comprise an exhaustive list. LP, LA, CP$^\pm$, CA$^\pm$ refer to linear polarizer, linear analyser, circular polarizer ($\pm$) and circular analyser ($\pm$), respectively.

Table 1. Resonances observed in the longitudinal beam

Resonance curve	Time dependence	Conditions of observation
A	unmodulated	LP or LA or both or neither
superposition of A and F	unmodulated	CP$^\bullet$ and CA$^\pm$ or no A
D	$\cos 2\omega_0 t$	LP or LA or both
E	$\sin 2\omega_0 t$	LP or LA or both
F	unmodulated	CP$^\pm$, separate monitoring beam with CP$^\mp$

Experimental recordings of typical D and E curves are compared with theoretical curves in figure 2. A discussion of the dependence of these curves on the parameters is given in section 3.4.

3.3.2. *Monitoring in the x direction.* The special interest of this arrangement lay in the generation of the functions χ' and χ'' by the use of a circular polarizer. These functions were only found for a polarized sample. They were not present in an aligned sample, nor when a linear polarizer was used for monitoring. The resonances observed were found according to table 2.
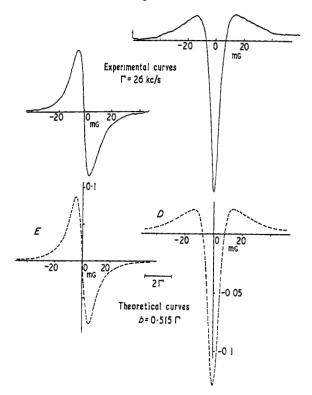
Figure 2. Experimental recordings of the amplitude of modulation at $2\omega_0$ (D and E functions) compared with theoretical curves. Experimental conditions: no polarizer, linear analyser, $\omega_0/2\pi = 0.5$ kc/s, $\Gamma = 26$ kc/s, $b/\Gamma = 0.515$.

Table 2. Resonances observed in the transverse beam

Resonance function	Time dependence	Polarizer in pumping beam	Polarizer in monitoring beam
χ' χ''	$\cos \omega_0 t$ $\sin \omega_0 t$	CP	CP
No signal	$\cos \omega_0 t$ $\sin \omega_0 t$	LP	CP
B C	$\cos \omega_0 t$ $\sin \omega_0 t$	CP or LP	LP
D E	$\cos 2\omega_0 t$ $\sin 2\omega_0 t$	CP or LP	LP

3.4. Fitting of resonance curves and determination of the damping constant

The parameter of the resonances which could not be measured directly was Γ, the damping constant. Its value is interesting in that it provides a measure of the lifetime of the metastable atoms, but in the context of the present experiments a more important consideration was to determine (i) how closely individual resonance curves could be fitted to the analytical functions using some particular value of Γ, and (ii) whether one and the same value of Γ could be used consistently for all the resonance functions. We shall treat these aspects separately.

It is necessary first to consider the factors which influenced the value of Γ. These were the pressure of gas in the cell, the discharge intensity and the intensity of the pumping light. In the comparisons in §§ 3.4.1 and 3.4.2 below, it is to be understood that these factors are held constant. In § 3.4.3, we consider the dependence of Γ on the intensity of the pumping light.

3.4.1. *The function* D. The amplitude of modulation at the peak of the resonance, D_0, was measured as a function of b ($=\gamma H_1$, where H_1 is the amplitude of the rotating field). Plots were made of $D_0(b)/D_0$ ($b \to \infty$) against b and compared with the theoretically derived curve plotted against b/Γ. The curves could be brought into coincidence by adjustment of the abscissae, thus allowing a determination of Γ. Examples of this fitting are shown in figure 3 (a).
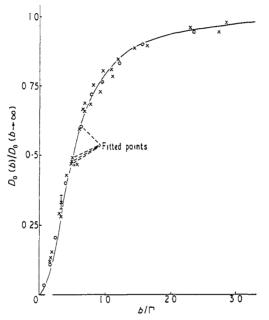

Figure 3(a). $D_0(b)/D_0(b \to \infty)$ as a function of b/Γ. Points correspond to experiments under different discharge conditions covering the range of Γ specified in tables 3 and 4. × and ○ refer to samples at 0·3 and 0·1 mmHg, respectively. The full curves are theoretical curves.

The width at half-intensity of the central feature, $\Delta_{1/2}$, was measured as a function of b. Plots were made of $\Delta_{1/2}$ against b, and compared with the theoretically derived curve of $\Delta_{1/2}/\Gamma$ against b/Γ. The curves could be brought into coincidence by adjustment of the ordinates and abscissae, using the same scale constant for each. Examples of this fitting are shown in figure 3 (b).

The values of Γ derived from fitting the curves of D_0 and $\Delta_{1/2}$ are independent of one another and are compared in table 3. Values of Γ in different rows must not be compared, since the intensity of the pumping light was different in each case.

The value of Γ used as a scale constant in figure 2 was the appropriate $\Gamma(D_0)$.

From the evidence of figures 2 and 3 and table 3 it is clear that the experimental curves are well represented by the function D.

3.4.2. *The function* E. The theoretical plot of E in figure 2 was drawn using the same

Table 3. Comparison between values of Γ derived from the amplitude D_0
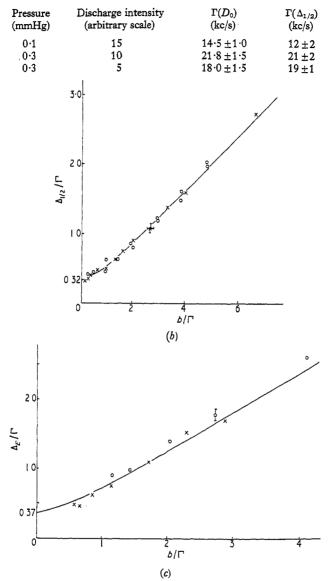and the linewidth $\Delta_{1/2}$

Pressure (mmHg)	Discharge intensity (arbitrary scale)	$\Gamma(D_0)$ (kc/s)	$\Gamma(\Delta_{1/2})$ (kc/s)
0·1	15	14·5 ±1·0	12 ±2
0·3	10	21·8 ±1·5	21 ±2
0·3	5	18·0 ±1·5	19 ±1

(b)

(c)

Figure 3. (b) $\Delta_{1/2}/\Gamma$ as a function of b/Γ. (c) Δ_E/Γ as a function of b/Γ. For details
see caption to figure 3(a).

scale constant as for D. The scale of the magnetic field is the same for the experimental
curves D and E, but the ordinates have been adjusted separately. The agreement between
the experimental and theoretical curves is striking.

The separation between the peaks of E, Δ_E, was measured as a function of b. Δ_E/Γ was
plotted against b/Γ using the appropriate value of $\Gamma(D_0)$, and was compared with the
theoretically derived plot. The result is shown in figure 3 (c). The agreement between

the experimental points and the theoretical curve is satisfactory evidence that the same value of Γ can be used consistently in D and E.

The same value of Γ was used also in analysing the resonance curves taken at $4\omega_0$ (§3.5).

3.4.3. *The intensity of the pumping light.* It is of particular interest to notice the dependence of Γ on the intensity of the pumping light. Table 4 shows values of $\Gamma(D_0)$ derived from one cell under different conditions of illumination for two different discharge conditions. For each discharge condition resonance curves were obtained (*a*) with the polarizing film in front of the cell and (*b*) with the film behind it. In cases (*b*) the light falling on the sample is more than twice as intense as in cases (*a*). Resonance curves of the same type were obtained for (*a*) and (*b*), but different values of Γ, as indicated in the table, were needed to secure a fit.

Table 4. Dependence of Γ on the intensity of the pumping light

Discharge intensity (arbitrary scale)	Position of polarizer	Γ (kc/s)	Discharge intensity (arbitrary scale)	Position of polarizer	Γ (kc/s)
5	(*a*) before	16 ± 0.7	10	(*a*) before	20.3 ± 0.7
5	(*b*) after	18 ± 1.5	10	(*b*) after	26.0 ± 1.5

These figures indicate that the contribution of optical pumping to the relaxation processes was noticeable, but not dominant.

3.5. *Observation of β processes*

Resonance effects were classified as β processes when the use of a linear polarizer in the pumping beam was essential to their production. The effects studied in detail were resonances in the longitudinal beam showing modulation at $4\omega_0$. A number of spurious effects causing modulation at this frequency were eliminated (§ 3.1.2).

Modulation at higher frequencies is predicted by the theory, as well as the modulation at $4\omega_0$. No systematic study of the higher frequencies was attempted, though it was established that modulation at $6\omega_0$ was present.

3.5.1. *Modulation at $4\omega_0$.* The signals appeared in the pumping beam by the use of a linear polarizer either with or without a linear analyser.

The modulation could be expressed by

$$S \cos 4\omega_0 t + T \sin 4\omega_0 t \tag{2}$$

where the strong signal S was represented by a bell-shaped resonance curve and the much weaker signal T by an antisymmetrical resonance curve. Typical experimental curves are shown in figure 4.

The result predicted by the theory for these resonance curves consists of a sum of terms whose relative weight depends on the spectral distribution of the light. The net result cannot therefore be precisely evaluated, but its general form can be deduced. It is

$$(F + KP) \cos 4\omega_0 t + KQ \sin 4\omega_0 t \tag{3}$$

where F is the function we have used before, P is a symmetrical and Q an antisymmetrical resonance function, and K is proportional to the intensity of the pumping light. The contribution F comes from one cycle of optical pumping, while P and Q require two cycles.

Of the functions which constitute P and Q, the products $(1-2A)F$ and DE have been selected as a suitable basis for comparison with experiment. The experimental curves can, in fact, be fairly well represented by these functions, but this does not imply that the other constituents of P and Q do not also contribute. Nor is it excluded that contributions from three or more pumping cycles may be present.
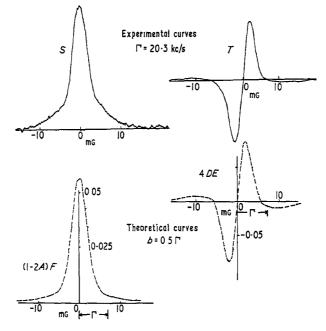

Figure 4. Experimental recordings of the amplitude of modulation at $4\omega_0$ (S and T functions) compared with theoretical curves (($1-2A)F$ and DE functions). Experimental conditions: linear polarizer, no analyser, $\omega_0/2\pi = 0.5$ kc/s, $\Gamma = 20.3$ kc/s, $b/\Gamma = 0.5$. The gain employed in recording the T function was ten times that employed for the S function.

3.5.2. *The function* S. The amplitude of modulation at the peak of the resonance, S_0, was measured as a function of b. Plots were made of $S_0(b)/S_0$ ($b\rightarrow\infty$) against b/Γ using the value of Γ derived from analysis of the function D. These curves were compared with corresponding plots derived from the theoretical functions F and $(1-2A)F$ (figure 5 (a)). The agreement is better with $(1-2A)F$.

The width at half-intensity, Δ_S, was measured as a function of b. Plots were made of Δ_S/Γ against b/Γ and compared with corresponding plots derived from F and $(1-2A)F$ (figure 5 (b)). The agreement is again better with $(1-2A)F$.

3.5.3. *The function* T. The weakness of the signal T led to difficulties in obtaining an experimental recording free from admixture with the much stronger quadrature component S. The intensity of T relative to S was greater at lower values of b, and the best curves were obtained under these conditions. The experimental curve in figure 4 shows good correspondence to the theoretical curve, for which the value of Γ obtained from the analysis of D has been used.

3.5.4. *Dependence on* ω_0. It is predicted on theoretical grounds that the strength of the
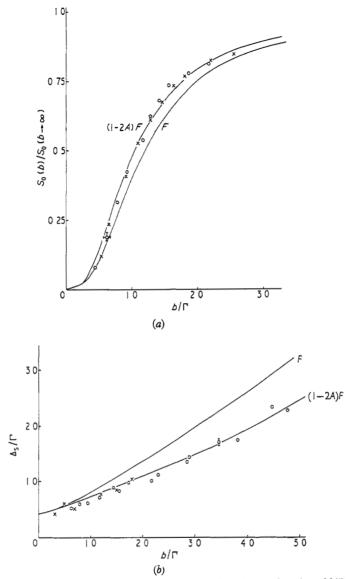
Figure 5. (a) $S_0(b)/S_0$ ($b \to \infty$) as a function of b/Γ. (b) Δ_s/Γ as a function of b/Γ. The points represented by × and ○ correspond to two different discharge conditions with $\Gamma = 16\ 0$ and $14\cdot5$ kc/s respectively. The full curves are theoretical curves derived from the functions F and $(1-2A)F$.

β processes should decrease as ω_0 is increased in relation to Γ. Accordingly, the amplitude S_0 was studied as a function of frequency. In order to avoid difficulties connected with the frequency response of the apparatus, S_0 was measured relative to D_0 generated at the frequency $\omega_0' = 2\omega_0$. The two resonance signals were thus compared at the same frequency $4\omega_0$. In these experiments the discharge conditions were kept constant. The D and S signals both tend to a maximum as b is increased. The value of b used in each case was large enough to attain this maximum.

D_0 was chosen as a reference signal because, at the time when the experiment was performed, it was believed that D_0 was independent of ω_0. According to the theory (which was at that time not fully developed), D_0 should indeed be independent of ω_0 if it is generated with an analyser but no polarizer, but not with the converse arrangement which was the one used in these experiments. The theoretical result for this case is

$$D_0 \, (b \to \infty) = \text{const.} \left(1 + \frac{\Gamma^2}{\Gamma^2 + 16\omega_0^2}\right)$$

$$= \text{const.} f(\omega_0)$$

where we have incorporated the relation $\omega_0' = 2\omega_0$. The experimentally determined ratio $S_0 \, (b \to \infty)/D_0 \, (b \to \infty)$ therefore needs to be corrected by the factor $f(\omega_0)$. The ratio $[S_0 \, (b \to \infty)/D_0 \, (b \to \infty)]_{\text{exp}} f(\omega_0)$ is plotted in figure 5 (c).
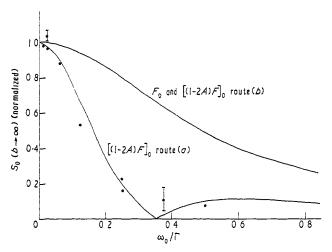

Figure 5(c). $S_0(b \to \infty)/D_0(b \to \infty)$ (corrected for the frequency dependence of D_0) as a function of ω_0/Γ. The points represent one set of experiments with $\Gamma = 20\cdot3$ kc/s. The full curves are theoretical curves showing the frequency dependence of F_0, $[(1-2A)F]_0$ by route (a) and $[(1-2A)F]_0$ by route (b).

For comparison with the experimental points theoretical curves are also plotted showing the frequency dependence of F_0 from the first-order solution, of $[(1-2A)F]_0$ from the second-order solution by route (a), and of $[(1-2A)F]_0$ from the second-order solution by route (b) (see figure 2 of I). In each case the condition $b \to \infty$, which leads to a great simplification, has been incorporated. The functions are

for F_0: $\qquad \dfrac{\text{const.}}{\Gamma^2 + 4\omega_0^2}$ $\hfill$ (4)

for $[(1-2A)F]_0$ by route (a): $\qquad \dfrac{\text{const.}(\Gamma^2 - 8\omega_0^2)}{(\Gamma^2 + 16\omega_0^2)(\Gamma^2 + 4\omega_0^2)}$ $\hfill$ (5a)

for $[(1-2A)F]_0$ by route (b): $\qquad \dfrac{\text{const.}}{\Gamma^2 + 4\omega_0^2}.$ $\hfill$ (5b)

The most significant point to notice is that the experimental points do not fit the first-order solution (4). They fit the second-order solution (5a) reasonably well.

3.6. *Discussion of the modulation at* $4\omega_0$

From the existence of the T signal and the evidence of the field and frequency dependence of the S signal, it is clear that the modulation at $4\omega_0$ cannot be attributed solely to the first-order solution F. The dominant component of the S signal must be attributed to second- or higher-order solutions, that is, to atoms which have undergone two or more complete cycles of optical pumping before the final interaction with the radio-frequency field and absorption of light.

It is anomalous that a stronger signal should arise from second- than from first-order processes. The fact that a second-order signal appears to be dominant has not been quantitatively explained, but a possible explanation lies in the fact that some components of the second-order signal are in antiphase with the first-order signal, and partially suppress it. In particular, the signal $(1-2A)F$ by route (b) occurs in antiphase with F and has the same dependence on frequency (compare the expressions (4) and (5b)). If there were approximate cancellation between these components of the signal, one could reconcile the theoretical curve $[(1-2A)F]_0$ by route (a) of figure 5 (c) with the experimental points. One would expect to find second-order signals of strength comparable with those in first order when the relaxation due to optical pumping became comparable with the relaxation due to other causes. The observation of line-broadening due to the pumping light (§ 3.4.3) is evidence that the experiments were conducted under such conditions.

4. Conclusions

The principal magnetic resonance phenomena (α processes) to be expected for a spin 1 system have been observed in absorption from the optically pumped level $2\,^3S_1$ in helium. The observations go beyond what has previously been studied in the comparable case of emission from the level $6\,^3P_1$ in mercury in that, with a suitable geometrical arrangement, the Bloch magnetic functions were observed.

The damping constant in terms of which the curves were interpreted varied with discharge conditions. It also varied with the intensity of the pumping light, pointing to some contribution from the optical pumping to the relaxation of the atoms. The smallest damping constants observed were in the region of 15 kc/s, corresponding to resonance linewidths of the order of 5 mG.

Modulation was also found at $4\omega_0$ under conditions which allowed its identification as a β process, that is, one in which atoms are left in a superposition state after one or more cycles of optical pumping. The symmetry of the resonance signals and their behaviour under variation of the frequency and strength of the inducing field lead to the conclusion that the dominant contribution to these signals is attributable to atoms which have undergone more than one complete cycle of optical pumping.

The observation of modulation at $4\omega_0$ is of particular interest in that it provides additional evidence for the circulation of coherence in optical pumping cycles.

grateful to them for making their experience and results available to us, and for stimulating our interest in these problems.

References

BROSSEL, J., and BITTER, F., 1952, *Phys. Rev.*, **86**, 308–16.

COHEN-TANNOUDJI, C., 1962, *Ann. Phys.*, *Paris*, **7**, 423–61, 469–504.

COLEGROVE, F. D., and FRANKEN, P. A., 1960, *Phys. Rev.*, **119**, 680–90.

DODD, J. N., SERIES, G. W., and TAYLOR, M. J., 1963, *Proc. Roy. Soc.* A, **273**, 41–68.

KIBBLE, B. P., and SERIES, G. W., 1963, *Proc. Roy. Soc.* A, **274**, 213–24.

PARTRIDGE, R. B., and SERIES, G. W., 1966, *Proc. Phys. Soc.*, **88**, 983–93.

ROSINSKI, K., 1964, *Bull. Acad. Pol. Sci.*, **12**, 497–502.

SCHEARER, L. D., 1961, *Advances in Quantum Electronics*, Ed. J. R. Singer (New York: Columbia University Press).

SERIES, G. W., 1966, *Proc. Phys. Soc.*, **88**, 957–68.

SKALINSKI, T., and ROSINSKI, K., 1964, *Z. angew. Math. Phys.*, **16**, 15.